Kalman Bass

4/29/2026

GEOL 394

Lithium Diffusion Experiments on Grossular Garnet

Advisors: Sarah Penniston-Dorland, Phillip Piccoli

Scientific Abstract:

This paper describes experiments in lithium diffusion profiles in grossular garnets to determine the effectiveness of those measurements as a way of constraining timescales of metamorphic fluid flow events through rocks. Metamorphic fluid drives chemical cycling and is a primary method of exchanging ions between rocks which causes metamorphism during a fluid flow event. A metamorphic fluid flow event is when a rock is exposed to metamorphic fluid. Metamorphic fluid flow events occur at a short duration relative to the geologic timescale, which means it has been difficult to determine the timescales of these events. One potential method of determining fluid flow event timescales is by measuring diffusion profiles of the ions they carry through rocks. Specifically, lithium ions and garnets were used for the experiments. Lithium is a rapid diffuser and has been shown to diffuse into garnets both in natural and synthetic samples. Garnet preserves chemical zoning and is abundant in metamorphic rocks. Grossular garnet is an end member of garnet where the +2 cation site is primarily occupied by a calcium cation. The diffusion method of lithium into garnet has not yet been determined, and these experiments were used to test the diffusivity of lithium into grossular garnet. A two-site diffusion mechanism is assumed to be the primary method of diffusion in this case. For these experiments, grossular garnet samples were exposed to powdered spodumene, a pyroxene mineral which acts as a lithium source, at a high temperature to stimulate the diffusion of lithium ions. After exposure, the concentration of lithium across depth into the samples were measured using laser ablation inductively coupled plasma mass spectrometry (LA-ICPMS). That data was modeled originally using a single-site diffusion equation as well as a two-site diffusion equation afterward. The results of these experiments were compared to results of similar experiments conducted using other garnet end members. The comparison of both diffusivity values showed there was no significant difference in diffusivities between grossular garnet and another garnet species.

Plain Text Abstract:

One of the most important aspects of metamorphism in rocks is the presence of metamorphic fluid in and around the rocks. This fluid is what drives chemical cycling and the movement of mass from one rock to another. Rocks are exposed to metamorphic fluid during fluid flow events which last a very short amount of time on a geological scale, and because of this it has been difficult to analyze periods of high fluid flow through rocks. However, it is possible to track the effects of fluid flow events by measuring concentration of ions that the fluid event leaves behind within the rocks it passes through. More specifically, diffusion profiles which plot concentration of lithium over depth within garnets can be measured because lithium can diffuse quickly into garnet without the concentrations without changing after the exposure. Lithium diffusion in garnet has not been explored until recently. These experiments are designed to stimulate diffusion of lithium within grossular garnet, a calcium-rich form of garnet, to later be measured, modeled against a diffusion equation, and compared to garnets with other chemical compositions. Originally, it was hypothesized that the lithium cations directly substitute with the calcium cations as they diffuse deeper into the garnet samples, meaning the grossular garnet would have at least one lower diffusivity value compared to other garnets. However, results of these experiments, when compared to results of similar experiments done on other types of garnet, showed that there was no significant difference between either diffusivity values.

Introduction and Background:

Most metamorphic processes involve metamorphic fluid in some capacity. Understanding metamorphic fluid flow through rocks will provide insight into exploratory economic geological methods because metamorphic fluid has the potential to lead to ore deposit formation and would also help to better predict seismic events because high fluid content in rock can be linked to seismic activity. The way to measure how fluid interacts with rocks is by observing the change in the chemistry of the rocks. An illustration of a metamorphic fluid flow event in a subduction zone is seen in figure 1 from Ramos et al. (2020). Hydrated rock from the subducting slab reaches high enough temperature and pressure to undergo dehydration reactions. Fluid exits the rock and travels through the overlying rock and drives mass transfer within the rocks that it passes through. The goal of these experiments is to constrain a time scale for metamorphic fluid flow events through rocks. Fluid flow events are where rocks are exposed to fluids which drive the process of chemical cycling, change the rock's chemistry, and move mass through the rock. Fluid can also cause melting and volcanism.

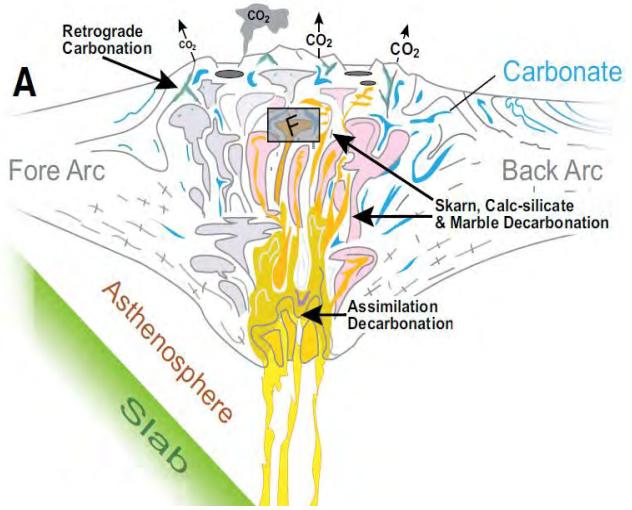


Figure 1, The path of fluid that causes decarbonation reactions in yellow. Fluid removes CO_2 from mineralogy, which escapes as a gas at the surface or gets reincorporated into the mineralogy with retrograde carbonation. (Ramos et al, 2020)

The reason that these experiments use lithium is that it is a fluid mobile element, meaning it can easily be picked up and deposited by metamorphic fluid. Lithium is also a fast diffuser, which will be beneficial when analyzing the results of these experiments due to their shortened timescale. Lithium diffusion has been observed within both natural and synthetic garnets (e.g. Penniston-Dorland et al.

2020). The lithium source for these experiments is powdered spodumene. Garnet is used in these experiments because it is a metamorphic mineral that preserves chemical zoning in some cases. Most natural garnets follow the following formula: $X_3Y_2(SiO_4)_3$, where the X site is occupied by a 2+ metal cation, usually Fe, Mg, Ca, or Mn, and the Y site is filled with a 3+ cation, in this case aluminum. The type of garnet used

Diffusivity is a property of an element in a mineral under specific conditions which identifies the rate at which materials move through areas of the mineral, it is measured in m^2/s. Measuring and modeling diffusion profiles of lithium into garnets can be used to track fluid flow events through rocks. The results from these experiments using a Ca-rich end member of garnet, along with similar experiments being performed by Hoff (2025) on different garnet end members will be used to help constrain the way lithium behaves within the garnet structure. These experiments will determine the effect, if any, that mineral chemistry has on the diffusivity of lithium into garnet. If one end member of garnet accepts lithium more rapidly than another, the difference between the two can be used to further develop an accurate time frame for fluid flow events interacting with garnet-bearing metamorphic rock.

Reynes et al. (2018) found that hydrogen diffusivity in grossular is different from spessartine, a Mn-rich end member. They found that H^+ ions require more energy to move between locations in grossular than locations in spessartine with the difference coming from size disparity of the 2+ metal cation of each type of garnet (Reynes et al., 2018). The ionic radius of Ca^{2+} being 1.06 angstrom and Mn^{2+} being 0.92 angstrom. Given that Li^+ and H^+ are both +1 cations, and both are rapid diffusers, it is expected that lithium will behave in a similar way. Goldschmidt's rules of ionic substitution within crystals dictate that ions will substitute more readily when their ionic radii are similar in size. Based on these, the hypothesis is that lithium will diffuse slower into grossular than any other end member of garnet. If there is no difference in diffusivity between garnet end members or diffusivity is higher in grossular, that means the diffusion of lithium is driven by other factors than just the 2+ metal cation.

The grossular garnet used for these experiments has a composition of 91.7% grossular, 6.1% spessartine, 1.9% almandine, and 0.3% pyrope analyzed by Will Hoover. It comes from the Jeffrey Mine in Asbestos, Quebec in Canada. The Jeffrey Mine was a major source of asbestos. It is in the Canadian Appalachians, 50 miles east of Montreal. The rocks there are a metamorphosed group of ophiolites from the seafloor in the Cambrian that have undergone several metamorphic and magmatic events (Wares and Martin 1980). That area is home to very calcium-rich rodingites, the source of the grossular samples. Rodingites are a product of high-pH fluid interaction with protoliths such as gabbro or serpentine to form metasomatized rocks that usually include elements that are left over from the serpentinization process (Wares and Martin 1980). They indicate that a rock must have been exposed to fluid and metamorphosed because of the fluid interactions. In this case, the rodingites from Jeffrey Mine started as felsic dyke rocks with high Si and Al and low Ca when analyzed using XRF (Wares and Martin 1980, Table 1, 288c) that were then exposed to major geologic processes and metamorphosed. The rocks that were rodingitized show a dramatic increase in calcium (Table 1: 1H, 1A, and 1G; Wares and Martin, 1980,). The rodingites underwent higher grades of metamorphism to form the several types of grossular garnet found in Jeffrey Mine including a deep green Cr-rich grossular, and the orange grossular used in these experiments. Their presence in the rock is evidence for a fluid-rock interaction at some point during their formation.

TABLE 1. BULK COMPOSITIONS OF RODINGITIZED FELSIC DYKE AND WALLROCK

	288c	1H	1A	1F	1G	1E	Harz.
SiO_2	61.61	56.84	53.66	39.89	53.60	51.77	41.55
Al_2O_3	14.22	12.51	13.18	13.06	1.68	5.43	0.31
FeO*	2.25	2.42	3.58	6.59	2.55	4.04	7.21
MgO	5.14	9.70	6.32	25.48	15.37	21.55	40.29
CaO*	7.44	13.65	17.43	2.72	25.57	13.15	0.34
Na_2O	3.74	0.26	0.11	0.08	0.54	0.18	0.06
K_2O	5.10	4.56	3.78	7.43	0.09	0.13	0.05
TiO_2	0.23	0.11	0.49	0.31	0.01	0.01	-
MnO	-	-	-	-	-	-	0.12
P_2O_5	0.11	0.11	0.11	0.21	0.09	0.06	-
H_2O (tot.)	-	0.20	1.59	4.82	0.18	4.36	9.48
total	99.84	100.36	100.25	100.59	99.68	100.68	99.31

288c: mildly rodingitized and Na-metasomatized felsic dyke rock. 1H: rodingitized felsic dyke rock in brecciated core zone. 1A: rodingitized felsic dyke rock at south edge of dyke. 1F: chloritic selvage (blackwall) at southern contact. 1G: rodingitized serpentinite (white rodingite, green halos around chromite grains. 1E: partly rodingitized serpentinite in hanging wall. * Total iron expressed as FeO. CaO values represent an average of XRF and AA determinations (XRF only for 288c and 1H). Harz.: 70% serpentinized harzburgite (Laurent 1975b).

Wares and Martin, Table 1; showing the bulk compositions of the rocks in Jeffrey Mine; sample 288c is the starting material; samples 1H, 1A, 1G, and 1E have been rodingitized at least

The diffusion method used for these experiments is the powder-source technique outlined in Watson and Dohmen (2010). During fluid flow events, the elements involved in chemical cycling are constantly being replenished by the flow of the fluid passing through the rock, and the concentration of

the dissolved components remain roughly the same. This could be considered a semi-infinite source of material, which means the experiment must simulate the same type of source. The lithium source for this experiment is a very finely ground spodumene, a Li-rich mineral. The lithium will diffuse into each of the garnet grains used in the experiment via the points of contact between the grains of spodumene and the surface of the samples. Even though there is not a continuous plane of contact, diffusion at the surface of the sample is easy, so the profile will even out as depth within the sample increases (Watson and Dohmen, 2010). Since each of the grossular garnet samples are surrounded completely by spodumene and isolated from each other, this is enough to simulate the semi-infinite source of lithium needed for the experiments. The reason a fluid source is not used is because fluid is too volatile. Each charge is sealed under a vacuum, and a fluid source of lithium could expand rapidly in intense heat and explode which would ruin the experiment.

It is possible to identify evidence of fluid flow events in metamorphic rocks using their chemical makeup, but it is difficult to constrain the length of time over which each of these fluid flow events took place. This is where the diffusion of lithium is useful. Penniston-Dorland et al., 2020, explored the diffusion of lithium in garnet baring rocks, and Marschall and Tang (2020) published an article that shows measurements of lithium isotope fractionation during diffusion can be used to determine accurate time scales for shorter geologic processes like fluid flow events. Lithium is an abundant, fluid-mobile element that readily and rapidly diffuses into many metamorphic rocks including garnets. The chemical zoning caused by the lithium diffusion into rocks is preserved once the rocks are “quenched” and become too cold to continue diffusion to equilibrium (Marschall and Tang, 2020). By studying the distance of lithium diffusion profiles in rocks, it is possible to constrain the lengths of these fast metamorphic processes including rapid fluid-flow events from dehydration reactions because the diffusion profiles will be preserved after “quenching” (Marschall and Tang, 2020). It is possible to calculate the time that the rock was in contact with the fluid if the diffusivity of the minerals within the rock is known.

The method of diffusion for lithium within garnet is not constrained yet, and the experiments have never been conducted before. Part of the long-term goals for this project is to be able to constrain a mechanism of diffusion for lithium within garnet. One of the theories for the way lithium enters the garnet chemical formula is via a single site coupled substitution of a lithium ion and a rare earth element with two of the ions within the 2+ metal cation site within the garnet chemical formula, meaning that one +1 lithium and a +3 rare earth element would substitute out for two 2+ metal cations. However, more than one mechanism of diffusion of lithium into garnet may be occurring, such as both coupled substitution as well as lithium occupying vacancies or interstitial zones within the chemical structure of the garnets. Dohmen et al (2010) shows that diffusion of lithium ions into olivine requires two methods to explain the diffusivity, and Hoff et al (2025) suggests the same thing is necessary to explain the diffusivity of lithium into pyrope-almandine garnets. Using a two-site diffusion equation model, if the values for the two diffusivities for grossular garnet are the same, then it can be assumed that there is only one mechanism of diffusion for lithium in grossular garnet. If one or both of the diffusivities of lithium in grossular garnet are the same as the diffusivities of lithium in pyrope-almandine garnet, that would suggest that at least one of the mechanisms for diffusion of lithium into garnet is not dependent on mineral chemistry.

Methods

The experiments began by selecting grains from the crystal aggregate of grossular. The grains were chosen to include the fewest number of fractures or inclusions which could change the rate of diffusion. Those grains were set in a dental resin plug and then polished using sandpaper along with a series of progressively finer grit diamond pastes. Once polished, grains were removed from the plug using acetone and cleaned in an ultrasonic cleaner. Pictures were taken of the polished grains using a reflected light microscope (Figure 2). The images show the polished face of the grains. Each grain was roughly

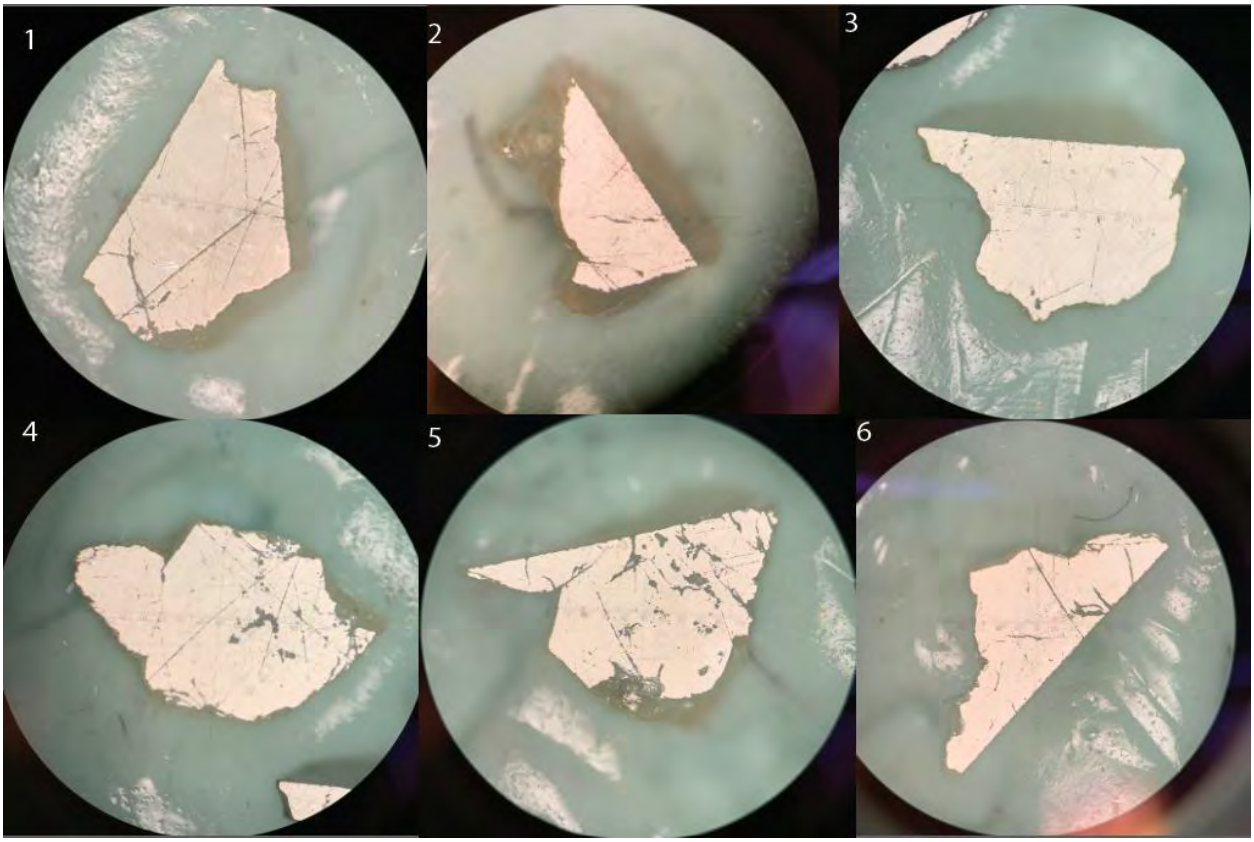


Figure 2, Images of Jgros 650 samples under a reflected light microscope at 5x magnification. The field of view is 2.7 mm in diameter.

between 2.5 and 2.3 mm along their longest axis so they would be able to fit into the experimental charges. Of the grains polished, the six cleanest were set aside for each of the diffusion experiments, and one grain was set aside to be analyzed as the starting material.

To prepare the experimental charges, tubes of fused quartz with an outer diameter of 7mm and an inner diameter of 3 mm were sealed on one end using an oxygen-methane flame. The tubes were then filled with the powdered lithium source, spodumene, and one of the grains set aside was then placed inside the tube with a polished face in contact with the surface of the spodumene powder. More spodumene was loaded into the tube, enough to cover the Jgros grain and to leave a margin of around 1 cm thick of powdered spodumene above the garnet grain to ensure there was enough material to simulate the semi-infinite source of lithium. The powdered spodumene and garnet were packed down and capped with a fused quartz spacer with a diameter of 3 mm, flush with the inner diameter of the tube. This process

was repeated once for each tube until each tube had two Jgros grains surrounded by spodumene. A vacuum was pulled in each tube to avoid any fluid being trapped within the furnace which could cause an explosion. Finally the charges were sealed under the vacuum.

Once the charges were made, they were loaded into a furnace. The first experiment had the furnace set to 650˚ C, and the charges were removed after a period of 2, 3, and 4 weeks. The second experiment was run at 750˚ C, and the charges were removed after 1, 2, and 4 weeks. The increase in temperature for the experiment was to address the potential effect of temperature on the diffusion of lithium within garnet. After the charges were removed, the Jgros samples were removed from the tubes by breaking the fused quartz open. The samples were then cleaned in the ultrasonic cleaner to remove any spodumene left on the grains and labeled by experiment (650 or 750), duration (1, 2, 3, or 4 weeks), and chamber within the charge (1 or 2). The labeled samples were photographed under the reflected light microscope, and the cleanest and least fractured sample from each charge as well as the starting material were set aside for analysis. The cleaning process for the second experiment failed, however, so samples from that experiment were then observed using the reflected light microscope and two of the samples were chosen to be scanned with backscattered electron microscopy (BSE).

The data for the first experiment was collected using laser-ablation inductively-coupled-plasma mass-spectrometry (LA-ICP-MS) using a depth profiling method (Smye and Stockli, 2014; Österle et al., 2019; Rasmussen et al., 2019) but had to be modeled as a function of depth rather than time. To convert the time steps of the laser firing into a depth profile, an estimated ablation rate of 0.7 µm per second was used. This ablation rate used was an estimate based on the ablation rate for one of the garnets analyzed by Christiana Hoff. An exact ablation rate was not determined for Jgros due to time constraints, which would affect the accurate depth used to model the diffusion equation. Data from six spots were measured for each duration. The data was first analyzed in Iolite, a software designed to visualize concentration data

measured using mass spectrometry (Paton et al. 2011). Then modeled in Excel to show a profile of concentration of lithium (in ppm) as a function of depth (in microns).

The data were then filtered for outliers using counting statistics. The count of lithium ions detected by the LA-ICP-MS were calculated using the equation $n = cps\ Li \times Dwell\ time$. Where cps Li is the counts per second of lithium detected in analysis and dwell time is the amount of time the LA-ICP-MS was measuring for lithium. Using the counts of lithium, the absolute uncertainty of the concentration was calculated using the equation: $abs\ uncertainty = {\sqrt{n}}/{n} \times Concentration\ of\ Li$. Where n was the counts of Li ions. Uncertainty for each datum was calculated using the above equation reported as 1-sigma (figure 3). Finally, the data was filtered out if a point along a profile deviated by more than 2-sigma from data at the corresponding and surrounding depth on the other profiles, the example shown has the filtered points circled.

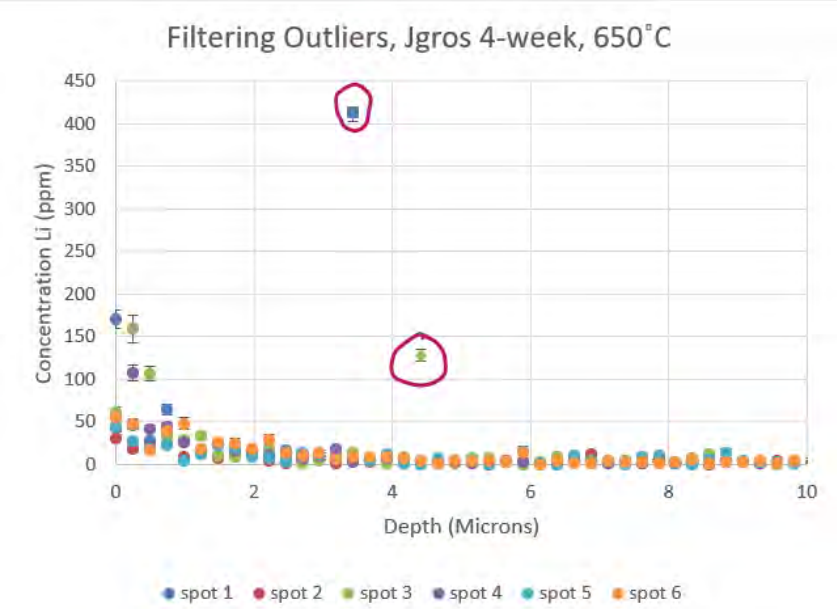


Figure 3, Outlier filtration. Measured concentration over depth data from LA-ICP-MS. Circled points are outliers that will be filtered out.

Once the measured profiles were filtered for outliers, a diffusion coefficient was calculated by fitting a diffusion equation based on Fick's Law of Diffusion to the measured concentration profile from each spot of analysis. The analytical solution of the diffusion equation used for this experiment assumes a semi-infinite source of lithium to simulate the fluid-rock interactions experienced by exhumed

metamorphic rocks, as well as a two-site diffusion method of lithium into garnet. The equation is $C = C_{S1} + (C_{i1} - C_{s1})erf\frac{x}{\sqrt{4D1t}} + C_{S2} + (C_{i2} - C_{s2})erf\frac{x}{\sqrt{4D2t}}$ (Zhang, 2010) where C is the measured concentration, Cs is the concentration of lithium in ppm on the surface of the sample in ppm, Ci is the internal concentration in ppm (Jgros starting material lithium concentration), erf is the error function, x is the depth within the sample in m, t is the duration of the experiment in s, and D is the diffusion coefficient in m^2/s (Zhang, 2010). A diffusion coefficient was calculated for every profile measured as well as an average diffusivity for each duration, and an overall diffusivity for each experiment.

Each of the diffusivity values were calculated using a MATLAB program by inputting a depth vector and measured data vectors as well as an input for the duration of the experiment as one of the constants. The program was given the two-site diffusion equation, the initial and boundary concentrations were pinned, and each of the D values were given a potential range. The calculations had to be done on the logarithmic scale. The program then was able to generate a best fit line for each of the depth profiles as well as an R-square value to determine the goodness of the fit. The modeling uncertainty was calculated by averaging the six D values from each duration and taking the standard deviation of the D1 and D2 for each spot of analysis from each duration separately. Then an overall average was calculated, and error was propagated using the addition error propagation formula: $\sqrt{(error\ A)^2 + (error\ B)^2 + (error\ C)^2}$. The overall diffusivity along with the modeled error were then compared to data from a similar experiment using a different garnet composition that was conducted by

Results

Ci1))-(erf(x/(2*sqrt((10^logD2)*t)))*(Cs2-Ci2))

Coefficients and 95% Confidence Bounds

	Value	Lower	Upper
Ci1	1.1088	NaN	NaN
Ci2	1.1088	NaN	NaN
Cs1	35.7991	32.0921	39.5061
Cs2	134.5025	129.2836	139.7214
logD1	-5.9694	-6.0622	-5.8766
logD2	-8.3520	-8.4447	-8.2594
t	2419200	NaN	NaN

Coefficients fixed at bound: Ci1, Ci2, t

Goodness of Fit

	Value
SSE	396.6359
R-square	0.9879
DFE	115.0000
Adj R-sq	0.9875
RMSE	1.8572

Figure 4, Example of the results section from the MATLAB modeling program. Log(D1) and Log(D2) values are the rows second and third from the bottom in the first table, R-square value is the second row from the top in the second table.

Christiana Hoff. Christiana's data includes average lithium concentration profiles for charges at 600˚ C and 700˚ C for a period of 2 and 3 weeks each.

Results

LA-ICP-MS data of the starting material revealed on average a linear concentration profile with Li concentrations below 3 ppm across 4 spots of analysis (see Appendix table 1). Data for the experimental run products of the 650˚ C experiment shows consistent evidence of diffusion curves with high concentrations of lithium at the surface that decrease non-linearly as depth increases across all 18 analyses for that duration. Figure 5 shows the 650˚ C 4-week average measured data versus the calculated diffusion profile based on that average. The models for each of the spots of analysis were calculated by anchoring the boundary concentrations and averaging the initial concentrations after about 15 microns

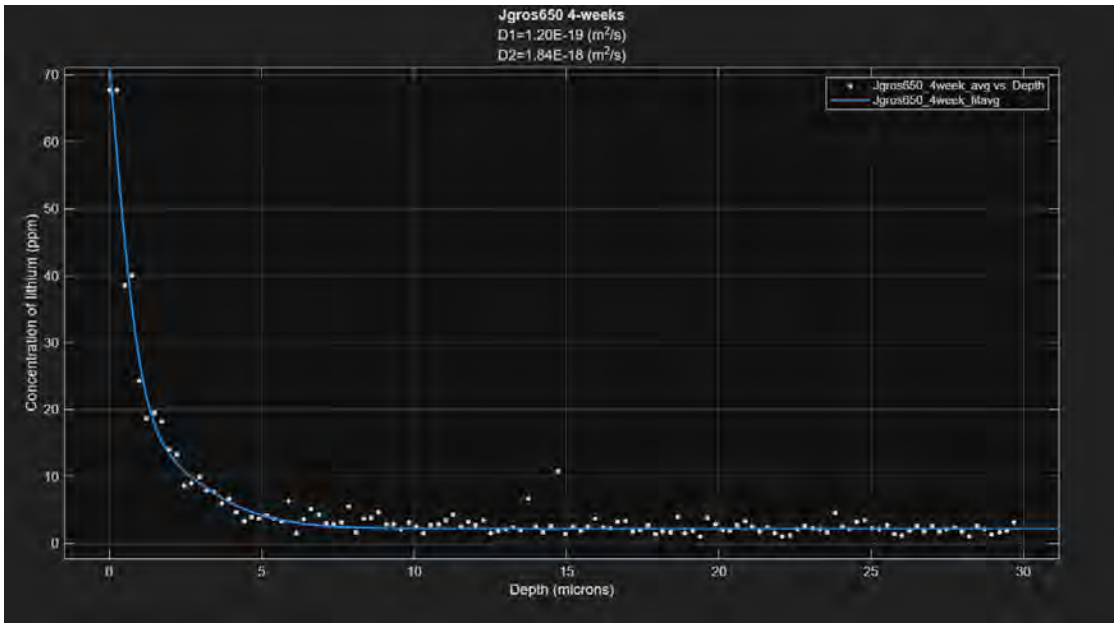


Figure 5, Comparison between measured average diffusion profile (white dots) and modeled diffusion profile (blue line).

within the garnet when the measured curve flattens out. The diffusivities varied from site to site along each sample, this is because of variations in surface conditions along the sample. Figure 6 shows the average D1 and D2 values across all 18 measurements as well as the standard deviation. A higher

diffusivity indicates faster diffusion, and all three D values fall within the same order of magnitude to each other. The error for the average D values was calculated as the standard deviation of the calculated D of each spot of analysis. The 3 average D each fall within 1-sigma of each other (Figure 6).

	D1 (m^2/s)	StDev D1	D2 (m^2/s)	StDev D2
2 week	3.51E-18	3.07E-18	1.81E-19	3.40E-19
3 week	3.65E-18	3.70E-18	4.94E-19	7.49E-19
4 week	2.90E-18	2.95E-18	2.46E-19	3.55E-19

Figure 6, Table of average D1 and D2 values and standard deviation (1-sigma) for 2, 3, and 4 weeks at 650° C

The samples for the 750° C experiment were not analyzed on the LA-ICP-MS. Reflected light microscope images of the samples extracted from the charges and cleaned revealed that the surfaces were clouded by a contaminant. The contaminant resisted ultrasonic cleaning as well as acetone baths and remained on the surface of the samples. Two of the six samples from the 750° C experiment were selected to be scanned using BSE. Figure 7 are the scans of the 2-week top sample and the 4-week bottom sample of the 750° C experiment. The scans of both samples reveal two distinct species on the surface of the grossular. One species covered less than 10% of the surface and had euhedral, tabular grains between 50 and 150 µm in length (Figure 7), while the other species covered over 90% of the surface and had very small anhedral crystals. The contamination was present across all six of the 750° C samples. The samples had to be analyzed using EDS to identify the two species and see if there was an intermediate phase between grossular and spodumene under high temperature low pressure conditions. Some hypotheses as to the source of the contamination that reacted inside the charges included residual putty from mounting samples under the reflected light microscope, human contamination like sweat left on the

surface of the samples, any new impurities within the fused quartz used for the charges, or any new impurities within the spodumene powder used as the lithium source.

While the 650˚ C experiment produced expected results and measurable diffusion profiles, the products from the 750˚ C experiment were unexpected. The BSE scans of the samples showed that little of the polished surface remained uncovered, meaning that there was no clean surface to analyze in LA-ICP-MS. The EDS data in figure 9 are from analysis of the larger, euhedral crystals on the surface of the samples. It shows spikes in Si and Al proportional to the chemical formula of spodumene, which also has a flat prismatic crystal habit. The larger, crystalline substance was most likely spodumene powder left on

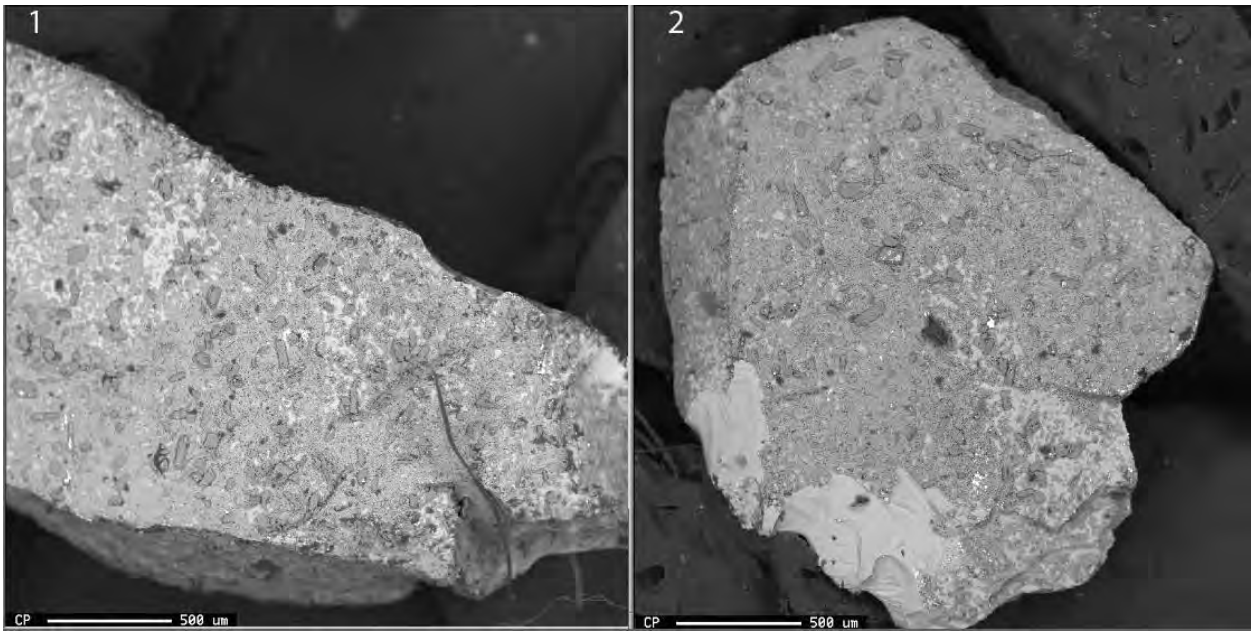


Figure 7, BSE scans of Jgros 750 samples, scale bar located on bottom. 7.1) Jgros 750 4-week bottom sample. 7.2) Jgros 750 2-week top sample.

the surface of the samples that resisted cleaning in both water and acetone in an ultrasonic cleaner. This did not occur on the 650˚ C experiment samples meaning that there could be a reaction between spodumene and garnet or a third substance at the higher temperature. Having a material high in lithium stuck to the surface of the samples when analyzing lithium concentrations in a mass spectrometer would skew the measurements for the whole analysis, so the experimental run products from the 750˚ C were

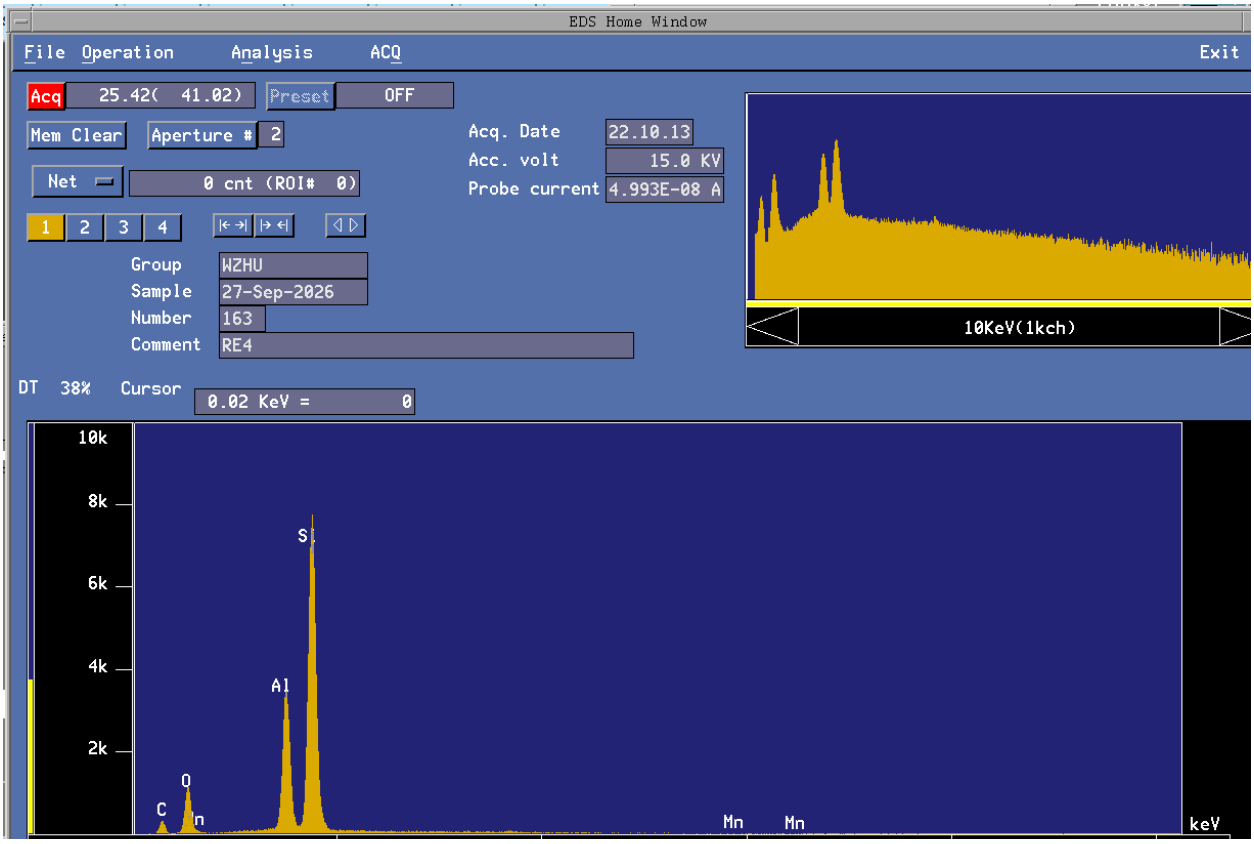


Figure 8, EDS scan of larger, tabular crystals on surface of Jgros 750 samples. Spikes at Si and Al are proportional to those of spodumene.

not analyzed for lithium diffusion profiles. The EDS data for the matte species on the surface of the samples as seen in figure 8 showed notable concentrations of both sodium and potassium oxides, neither

of which are found within the chemical formulae of Jgros or the spodumene powder used.

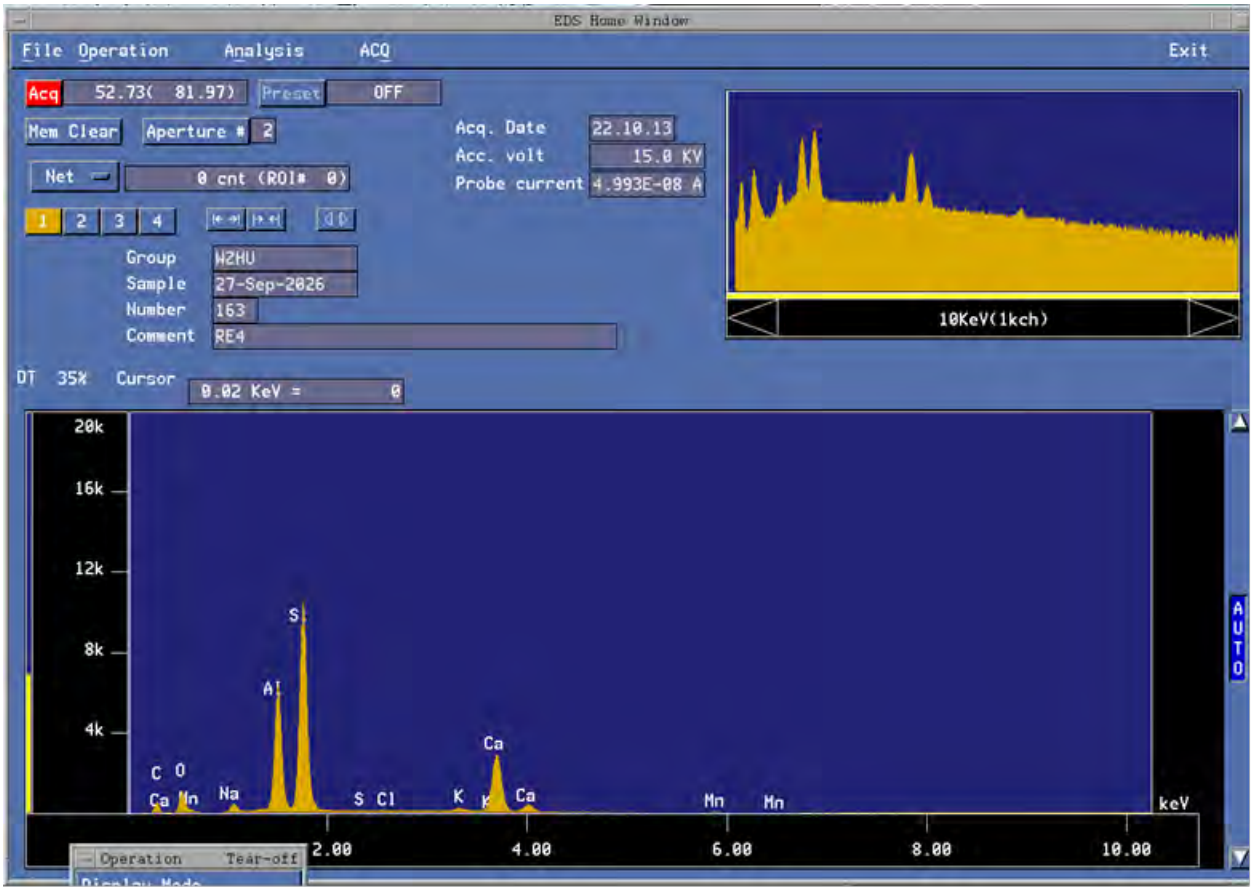


Figure 9, EDS data for matte substance on the surface of Jgros 750. Al, Si, and Ca are from grossular. Elements with unknown source are Na and K.

It is unlikely that these elements were precipitating from sweat left on the surfaces of the samples, since gloves were used while handling the samples and they were cleaned in an ultrasonic cleaner immediately before being sealed within the charges. The source could also have been the putty used to mount the samples under the reflected light microscope, however XRF data of the putty revealed that the weight % of potassium oxides within the putty was far too low at 0.0095% to contribute to the level of contamination measured. The source for the sodium and potassium bearing phase is unknown and requires more testing.

Discussion

The goal of these experiments was to test and model one potential method of lithium diffusion into garnet, specifically a calcium end-member grossular. The 650˚ C experiment showed results that diffusion occurred. Diffusion occurred over all the samples as compared to the initial baseline concentration of lithium within the starting material, and every depth profile was able to be modeled successfully to calculate diffusivities. The hypothesis for the experiments was that grossular would have higher diffusivity values with lithium when compared to other garnet species. Similar experiments were conducted by Christiana Hoff which collected lithium diffusion data within a pyrope-almandine collected from Gore Mountain in New York. Those experiments were run at 600˚ C and 700˚ C. Figure 10 compares the modeled diffusivities from the Gore Mountain pyrope-almandine with the average modeled diffusivities from the Jeffrey Mine grossular including the modeling uncertainty. Both the diffusivities for lithium in grossular at 650˚ C lie above the expected diffusivity of the GM garnet at that temperature, however the uncertainty for the diffusivities overlap even with the lower values of the Gore Mountain pyrope-almandine. This indicates that mineral chemistry does not significantly contribute to the diffusion of lithium within garnet.

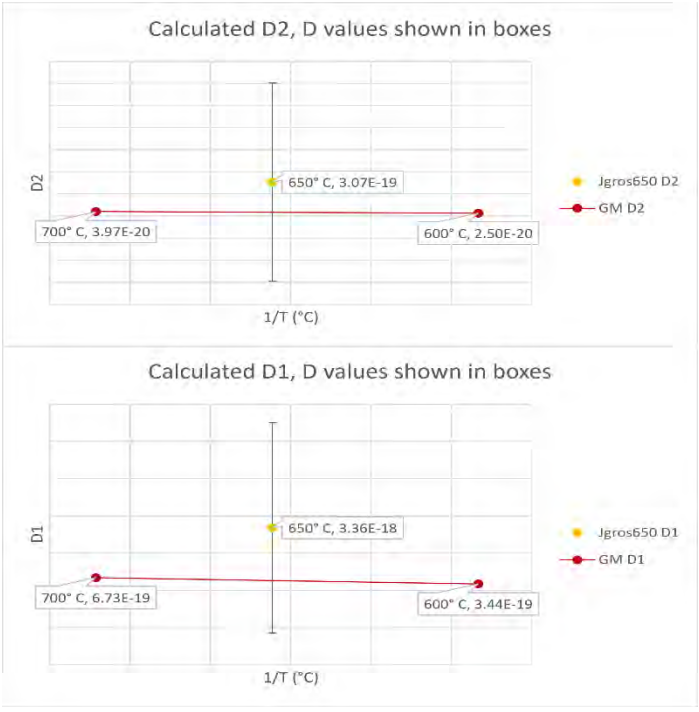


Figure 10, Arrhenius diagram comparing average D1 and D2 of Jgros 650 with error bars shown (Orange) and Gore Mountain Pyrope at 600 and 700 degrees (Red).

Conclusion:

Of the two experiments run for this project, one yielded results that could be analyzed, and the other had unexpected results that provided insight into the way these experiments were designed. The first experiment at 650˚ C showed measurable diffusion profiles across each of the samples as well as a general baseline concentration for lithium within the garnet itself. The diffusivities for each duration of the first experiment were all within one standard deviation of each other, and the overall diffusivity for that temperature was compared to diffusivities to another garnet with a different mineral chemistry closer to a pyrope. The D values for the grossular involved in these experiments were D1 = 3.36±5.64E-18 and D2 = 3.07±8.96E-19 which overlapped the range of the diffusivity values for the other garnet. The hypothesis for this experiment was that lithium would diffuse slower into grossular garnet than other garnet chemistries based on findings from experiments using hydrogen diffusivity out of grossular garnets compared to other garnets (Reynes et. al, 2018). The results from this project, however, do not support this hypothesis since the error of the grossular diffusivities overlap both D1 and D2 for the other garnet at similar temperatures. This could mean that diffusion of lithium within garnet is not dependent on garnet mineral chemistry. Since the method of diffusion for lithium within garnet is still undefined, these results could help further deduce that mechanism. It's unlikely, based on these results, that lithium replaces the +2-metal cation site in garnet to diffuse since otherwise the reaction between those ions would have more of an effect on the rate of diffusion.

Bibliography

Österle et al. 2019. "New age constraints on the Lan Sang gneiss complex, Thailand, and the timing of activity of the Mae Ping shear zone from in-situ and depth-profile zircon and monazite U-Th-Pb geochronology." *Journal of Asian Earth Sciences* 181.

Paton et al. 2011. "Iolite: Freeware for the visualisation and processing of mass spectrometric data." *Journal of Analytical Atomic Spectrometry.* doi:10.1039/c1ja10172b.

Penniston-Dorland et al. 2020. "Li isotope zoning in garnet from Franciscan eclogite and amphibolite: The role of subduction-related fluids." *Geochimica et Cosmochimica Acta* 286: 198-213.

Ramos, et al. 2020. "Remnants and Rates of Metamorphic Decarbonation in Continental Arcs." *The Geological Society of America.*

Reynes et al. 2018. "Experimental constraints on hydrogen diffusion in garnet." *Contributions to Mineralogy and Petrology* 1-23.

Smye, A., and D. Stockli. 2014. "Rutile U–Pb age depth profiling: A continuous record of lithospheric thermal evolution." *Earth and Planetary Science Letters* 408: 171-182.

Wares, R., and R. Martin. 1980. "Rodingitization of Granite and Serpentinite in the Jeffrey Mine, Asbestos, Quebec." *Canadian Mineralogist* 18: 231-240.

Watson, E., and R. Dohmen. 2010. "Non-traditional and Emerging Methods for Characterizing Diffusion in Minerals and Mineral Aggregates." *Reviews in Mineralogy and Geochemistry* 72: 61-105.

Zhang, Y. 2010. "Diffusion in Minerals and Melts: Theoretical Background." *Reviews in Mineralogy and Geochemistry* 72: 5-59.

Appendix:

	Li concentration (ppm) by spot number					
Depth (um)	1	2	3	4	average	Stdev
0.00	1.76	2.32	1.46	1.56	1.78	0.38
0.25	-0.56	2.32	0.67	3.01	1.36	1.61
0.49	2.62	1.28	3.03	2.11	2.26	0.75
0.74	1.23	0.45	2.89	0.70	1.32	1.10
0.98	1.76	-0.20	0.99	3.11	1.42	1.39
1.23	1.42	2.07	0.70	1.81	1.50	0.60
1.47	0.51	1.45	4.33	0.44	1.69	1.83
1.72	5.59	1.40	2.03	0.37	2.35	2.27
1.96	3.63	0.86	0.33	1.56	1.59	1.45
2.21	0.35	-0.19	2.51	1.41	1.02	1.20
2.45	-0.18	0.40	-0.32	1.10	0.25	0.64
2.70	1.96	-0.16	9.73	-0.23	2.83	4.71
2.94	0.46	1.27	0.99	0.27	0.75	0.46
3.19	0.34	0.27	0.46	1.16	0.56	0.41
3.44	0.80	2.46	3.26	1.14	1.92	1.15
3.68	0.35	0.45	1.65	0.62	0.77	0.60
3.93	0.36	2.50	1.06	1.35	1.32	0.89
4.17	1.36	2.11	0.21	2.83	1.63	1.12
4.42	1.39	2.26	0.76	1.32	1.43	0.62
4.66	-0.28	0.34	2.59	0.94	0.90	1.23
4.91	-0.18	0.54	3.01	0.23	0.90	1.44
5.15	-0.26	1.75	0.63	1.85	0.99	1.00
5.40	0.62	-0.21	-0.43	0.78	0.19	0.60
5.64	0.36	1.58	0.44	1.02	0.85	0.57
5.89	3.34	0.33	1.76	0.80	1.56	1.33
6.13	1.02	-0.21	0.28	3.32	1.10	1.56
6.38	0.36	0.57	2.82	0.58	1.08	1.16
6.63	2.03	-0.44	-0.49	0.31	0.35	1.18
6.87	2.96	1.12	-0.25	1.25	1.27	1.31
7.12	-0.20	1.90	2.19	2.20	1.52	1.16
7.36	0.85	2.62	0.56	1.69	1.43	0.93
7.61	1.68	1.63	1.60	0.45	1.34	0.59
7.85	-0.21	0.34	0.54	-0.18	0.13	0.38
8.10	1.29	0.29	0.43	4.16	1.54	1.80
8.34	-0.24	-0.24	-0.51	2.05	0.26	1.20
8.59	2.42	-0.43	4.09	1.88	1.99	1.87
8.83	1.96	0.33	-0.21	0.25	0.58	0.95
9.08	1.09	0.47	1.25	3.69	1.63	1.42
9.33	2.32	0.99	-0.41	0.53	0.86	1.14
9.57	0.27	1.02	0.61	0.82	0.68	0.32
9.82	-0.31	0.69	0.52	0.27	0.29	0.44

Appendix Table 1; Jgros Starting Material; Lithium concentration measurements (ppm) over depth (µm) for 4 spots, the average, and standard deviation of all 4 spots.

	Lithium Concentrations (ppm)							
Depth (µm)	1	2	3	4	5	6	average	stdev
0.00	123.88	82.72	74.18	75.12	42.72	124.28	87.15	31.73
0.25	56.16	25.63	71.16	60.75	34.94	67.05	52.62	18.28
0.49	32.73	13.77	52.84	41.15	37.67	27.82	34.33	13.18
0.74	37.10	31.42	36.64	29.88	43.15	19.03	32.87	8.25
0.98	47.70	36.82	32.54	40.38	39.97	55.20	42.10	8.12
1.23	19.94	16.28	26.74	28.88	25.24	29.13	24.37	5.18
1.47	18.41	12.03	31.19	19.86	20.19	23.55	20.87	6.32
1.72	15.09	11.79	33.13	19.05	29.77	13.75	20.43	8.92
1.96	19.06	14.52	16.57	21.79	9.71	38.46	20.02	9.93
2.21	14.32	4.95	23.25	16.91	14.37	15.17	14.83	5.89
2.45	13.44	0.77	15.47	10.54	14.79	15.04	11.67	5.64
2.70	10.16	7.31	11.97	36.90	6.96	7.90	13.53	11.61
2.94	7.66	14.89	11.44	11.58	8.31	13.98	11.31	2.91
3.19	7.30	4.75	4.94	7.54	13.63	7.12	7.55	3.22
3.44	10.61	2.04	4.55	6.22	12.24	7.14	7.13	3.78
3.68	1.74	8.84	8.45	9.51	6.46	7.23	7.04	2.82
3.93	3.53	7.32	5.69	9.78	10.04	12.09	8.07	3.16
4.17	3.11	1.34	5.25	12.51	10.24	8.10	6.76	4.29
4.42	3.77	0.30	8.26	4.43	9.78	3.51	5.01	3.45
4.66	1.28	6.10	7.74	9.03	10.36	4.67	6.53	3.27
4.91	2.44	10.93	2.90	6.61	4.88	4.55	5.38	3.10
5.15	6.53	3.14	2.46	7.44	8.16	6.20	5.66	2.33
5.40	2.71	-0.23	5.55	1.41	8.17	4.11	3.62	3.01
5.64	4.14	1.78	2.75	6.21	6.54	2.37	3.97	2.02
5.89	2.33	9.19	0.55	3.42	8.48	-0.37	3.93	4.03
6.14	5.36	3.18	1.62	6.36	7.72	3.58	4.64	2.25
6.38	4.95	2.88	2.22	6.61	2.17	1.01	3.31	2.08
6.63	2.51	1.32	6.86	4.36	3.24	4.45	3.79	1.91
6.87	3.83	5.77	1.04	3.15	1.54	8.47	3.97	2.78
7.12	1.27	8.50	3.54	4.04	4.64	12.05	5.67	3.91
7.36	1.79	1.06	2.86	1.73	6.57	1.61	2.60	2.03
7.61	2.81	2.11	9.98	3.35	1.25	2.94	3.74	3.15
7.85	1.47	1.27	2.65	3.62	1.75	4.42	2.53	1.27
8.10	-0.29	1.26	2.50	1.64	5.02	3.36	2.25	1.83
8.34	1.46	0.26	1.19	1.54	3.75	1.64	1.64	1.15
8.59	0.36	0.64	0.54	3.52	1.11	2.85	1.50	1.34
8.83	2.05	0.58	2.35	3.31	2.37	2.20	2.14	0.89
9.08	2.51	3.24	1.67	1.40	2.85	0.55	2.04	1.01
9.33	1.99	2.01	3.04	0.36	5.37	2.13	2.48	1.66
9.57	1.05	1.04	2.28	2.43	0.38	4.90	2.01	1.62
9.82	0.84	-0.67	0.50	4.59	-0.28	2.77	1.29	2.01
10.06	2.78	0.65	5.51	1.79	5.73	3.20	3.28	2.02
10.31	3.10	-0.25	6.75	3.57	1.30	1.48	2.66	2.43
10.55	-0.28	0.52	1.09	1.07	1.48	2.61	1.08	0.97
10.80	-0.26	1.89	2.82	2.16	2.85	4.18	2.27	1.47
11.04	0.75	-0.37	2.14	2.79	-0.35	3.37	1.39	1.61
11.29	0.58	1.82	3.25	4.39	3.26	0.45	2.29	1.60
11.53	0.48	1.94	5.70	2.61	1.59	3.66	2.66	1.83
11.78	0.98	5.98	1.45	2.52	4.51	2.58	3.00	1.90
12.02	1.34	0.69	2.38	2.07	0.94	3.12	1.76	0.93
12.27	2.26	-0.27	3.29	3.33	4.41	1.17	2.36	1.70
12.52	1.68	0.37	5.74	3.28	1.26	0.87	2.20	2.00
12.76	-0.21	5.07	2.07	2.12	1.41	2.58	2.17	1.72
13.01	1.88	3.28	0.66	2.73	5.17	2.39	2.69	1.51
13.25	0.74	0.31	2.69	5.11	3.03	1.15	2.17	1.80
13.50	1.61	1.00	2.02	1.83	1.10	1.80	1.56	0.42
13.74	1.08	6.47	2.52	4.57	1.15	2.07	2.98	2.13
13.99	3.73	2.07	2.23	0.42	4.61	4.15	2.87	1.58
14.23	3.99	-0.30	3.04	1.87	0.48	1.12	1.70	1.61
14.48	2.18	3.04	2.21	3.32	1.27	2.48	2.42	0.73
14.72	1.14	11.35	5.26	0.48	3.60	0.45	3.71	4.21
14.97	2.15	5.65	1.59	1.34	2.59	0.54	2.31	1.78

Appendix Table 2; Jgros ERP 2-weeks; Lithium concentration measurements (ppm) over depth (µm) for 6 spots, the average, and standard deviation of all 6 spots.

	Lithium Concentrations (ppm)							
Depth (µm)	1	2	3	4	5	6	average	stdev
0.00	93.64	110.62	24.95	15.91	59.65	29.27	55.68	39.24
0.25	25.60	48.85	57.36	30.88	27.03	28.18	36.32	13.39
0.49	24.19	30.69	40.82	30.02	31.91	33.23	31.81	5.40
0.74	19.62	19.20	27.80	19.08	26.50	41.63	25.64	8.74
0.98	28.62	22.74	11.23	24.91	19.48	22.04	21.50	5.89
1.23	16.31	13.63	33.02	31.19	18.46	20.70	22.22	8.03
1.47	7.23	15.83	13.21	15.39	14.41	26.67	15.46	6.32
1.72	5.47	7.06	9.09	28.14	26.37	12.41	14.75	9.97
1.96	18.47	10.85	9.13	14.36	25.55	10.05	14.73	6.32
2.21	9.35	23.22	9.98	11.39	11.40	7.30	12.11	5.65
2.45	4.83	11.27	11.28	7.92	17.62	11.49	10.74	4.28
2.70	6.39	9.50	5.46	12.20	14.79	6.09	9.07	3.79
2.94	0.56	8.96	3.69	6.45	12.97	6.41	6.51	4.27
3.19	2.77	15.59	6.64	11.87	16.44	0.81	9.02	6.61
3.44	4.73	5.58	13.13	8.14	14.91	9.93	9.40	4.06
3.68	1.42	9.36	11.05	10.64	11.31	6.85	8.44	3.81
3.93	8.31	11.34	7.00	6.07	8.23	1.70	7.11	3.19
4.17	3.86	10.47	4.94	10.26	9.05	7.05	7.61	2.78
4.42	2.61	1.50	9.23	7.17	11.00	2.05	5.59	4.08
4.66	4.58	1.85	2.38	4.44	9.37	4.52	4.52	2.66
4.91	2.59	7.16	4.81	3.38	13.86	4.06	5.98	4.17
5.15	5.10	6.76	8.44	11.63	7.45	2.04	6.90	3.22
5.40	0.39	0.97	5.38	6.10	3.83	3.61	3.38	2.30
5.64	2.46	3.47	4.61	5.66	11.57	2.71	5.08	3.40
5.89	3.39	3.07	2.55	5.49	10.98	1.36	4.47	3.46
6.13	1.39	4.00	5.98	7.09	5.43	3.77	4.61	2.01
6.38	0.98	1.68	3.93	5.47	8.17	2.83	3.84	2.66
6.63	1.85	0.42	1.32	2.43	9.74	4.59	3.39	3.41
6.87	2.88	2.61	2.46	3.66	6.65	0.63	3.15	1.98
7.12	1.33	7.86	3.58	4.59	6.72	1.14	4.20	2.75
7.36	3.18	0.62	-0.35	7.28	8.18	2.61	3.59	3.47
7.61	0.48	-0.37	1.95	4.01	12.38	1.21	3.28	4.70
7.85	1.34	5.09	2.65	7.55	5.74	2.59	4.16	2.35
8.10	-0.36	6.81	2.77	4.34	7.15	1.32	3.67	3.00
8.34	0.45	0.98	4.51	4.46	5.98	4.68	3.51	2.24
8.59	0.58	2.15	-0.42	3.86	3.91	1.30	1.90	1.76
8.83	2.25	8.76	0.53	3.62	1.63	2.46	3.21	2.90
9.08	0.57	0.51	2.69	11.00	8.91	1.71	4.23	4.55
9.33	1.27	0.65	0.52	3.79	-0.29	1.75	1.28	1.41
9.57	1.74	2.01	3.07	7.10	12.64	2.34	4.82	4.31
9.82	2.18	8.01	2.58	5.71	2.65	4.12	4.21	2.28
10.06	1.22	3.44	2.61	7.28	5.78	0.36	3.45	2.66
10.31	2.03	-0.30	4.92	8.50	4.81	1.12	3.51	3.19
10.55	1.20	3.08	-0.29	8.29	5.68	2.33	3.38	3.13
10.80	-0.27	-0.45	0.33	6.77	4.45	0.65	1.91	2.98
11.04	1.87	2.28	0.41	5.78	1.10	0.47	1.98	2.00
11.29	0.45	0.43	0.47	5.90	5.76	0.48	2.25	2.77
11.53	0.41	1.12	0.50	6.97	2.75	0.44	2.03	2.58
11.78	1.44	1.07	1.39	7.06	10.11	0.55	3.60	3.99
12.02	1.44	4.26	1.49	2.49	2.72	1.69	2.35	1.08
12.27	1.13	1.61	3.42	4.30	4.99	0.60	2.67	1.81
12.52	5.49	1.29	4.24	2.85	4.54	0.66	3.18	1.91
12.76	5.93	3.02	3.50	2.63	7.73	0.39	3.87	2.59
13.01	3.65	-0.40	1.35	4.61	1.96	1.99	2.19	1.76
13.25	3.47	0.53	0.53	6.56	4.81	1.40	2.89	2.48
13.50	2.67	0.98	3.73	3.67	10.87	1.57	3.91	3.58
13.74	1.92	0.46	0.41	4.61	5.72	2.08	2.53	2.18
13.99	2.66	1.86	1.19	4.60	2.64	0.76	2.29	1.37
14.23	3.78	1.00	-0.32	6.08	5.34	2.03	2.99	2.51
14.48	0.56	0.41	2.07	3.52	6.87	3.60	2.84	2.41
14.72	1.60	0.32	1.90	7.33	4.13	0.47	2.62	2.68
14.97	2.52	7.66	1.23	5.80	3.30	-0.29	3.37	2.93

Appendix Table 3; Jgros ERP 3-weeks; Lithium concentration measurements (ppm) over depth (µm) for 6 spots, the average, and standard deviation of all 6 spots.

	Lithium Concentrations (ppm)							
Depth (µm)	1	2	3	4	5	6	average	stdev
0.00	170.30	31.00	61.79	43.29	45.24	54.62	67.70	51.34
0.25	46.58	18.53	159.44	107.94	26.90	47.25	67.77	54.74
0.49	28.37	19.75	106.81	41.99	17.76	17.05	38.62	34.71
0.74	64.63	36.70	32.46	43.96	23.13	39.38	40.04	13.97
0.98	27.59	9.03	29.76	25.50	5.30	48.24	24.24	15.55
1.23	17.44	15.10	33.77	14.77	12.26	18.92	18.71	7.73
1.47	23.24	7.68	11.46	25.15	23.15	26.19	19.48	7.85
1.72	23.10	14.56	9.68	16.12	20.56	25.26	18.21	5.82
1.96	16.76	10.81	15.34	13.67	9.32	17.79	13.95	3.34
2.21	9.87	4.10	18.16	10.25	8.15	28.90	13.24	8.93
2.45	16.51	2.11	7.71	9.36	2.49	13.56	8.62	5.80
2.70	12.42	6.84	0.75	8.27	14.06	11.39	8.96	4.82
2.94	8.52	7.49	5.23	11.41	12.49	14.50	9.94	3.45
3.19	5.66	1.39	10.93	18.34	5.34	5.70	7.89	5.95
3.44	413.64	4.00	13.78	2.70	9.12	8.72	75.33	165.79
3.68	6.62	3.75	5.27	4.95	5.04	9.73	5.89	2.09
3.93	2.81	4.67	1.58	7.91	12.95	9.82	6.62	4.37
4.17	-0.30	3.27	9.15	6.30	1.32	8.35	4.68	3.85
4.42	4.23	2.35	128.24	4.05	0.57	5.16	24.10	51.05
4.66	1.90	1.01	4.91	6.67	6.88	2.15	3.92	2.57
4.91	3.49	4.07	1.64	3.49	4.96	4.56	3.70	1.17
5.15	2.81	2.81	8.17	0.78	6.09	4.07	4.12	2.64
5.40	0.45	4.09	7.00	4.14	1.17	4.99	3.64	2.44
5.64	2.59	5.24	2.33	2.48	3.63	3.53	3.30	1.10
5.89	2.23	3.24	0.40	3.12	14.90	14.22	6.35	6.44
6.14	1.18	2.37	2.98	0.44	1.30	0.64	1.48	1.00
6.38	0.45	3.02	9.27	2.95	0.69	4.74	3.52	3.24
6.63	3.77	3.84	4.48	5.50	10.76	1.93	5.05	3.03
6.87	0.80	12.19	3.90	3.63	2.74	2.00	4.21	4.07
7.12	0.97	1.54	5.05	1.91	3.85	4.05	2.89	1.64
7.36	3.85	1.47	4.35	3.29	0.60	3.11	2.78	1.45
7.61	-0.41	2.09	2.07	1.96	8.91	3.58	3.03	3.15
7.85	5.53	3.70	4.80	6.09	11.16	1.85	5.52	3.15
8.10	2.23	1.31	-0.39	2.26	1.51	2.60	1.59	1.09
8.34	3.08	0.72	7.32	3.19	0.52	6.86	3.61	2.92
8.59	0.59	0.57	12.50	1.84	5.97	1.40	3.81	4.71
8.83	4.44	2.33	2.30	2.43	13.05	3.00	4.59	4.22
9.08	2.28	3.39	4.26	-0.40	5.00	2.67	2.87	1.89
9.33	1.12	1.64	4.21	2.09	2.87	4.82	2.79	1.47
9.57	2.59	3.82	0.60	-0.34	3.54	2.23	2.07	1.64
9.82	2.84	4.19	3.50	1.47	2.00	4.17	3.03	1.13
10.06	2.34	1.53	2.05	6.25	0.46	2.12	2.46	1.98
10.31	0.50	1.65	0.48	1.87	3.03	1.73	1.54	0.96
10.55	0.52	4.08	1.61	2.36	4.27	3.06	2.65	1.45
10.80	2.63	1.53	2.03	5.80	1.79	3.27	2.84	1.58
11.04	2.48	4.39	2.67	5.20	3.80	2.09	3.44	1.22
11.29	-0.30	7.29	6.94	2.57	4.94	4.12	4.26	2.84
11.53	0.56	2.30	2.58	3.52	3.57	2.37	2.48	1.09
11.78	2.48	4.51	0.55	1.94	7.06	2.86	3.23	2.27
12.02	1.47	4.03	2.45	6.15	0.55	1.90	2.76	2.03
12.27	0.61	3.31	5.60	1.84	5.81	3.38	3.42	2.04
12.52	0.50	0.67	3.12	-0.29	1.90	3.41	1.55	1.51
12.76	1.72	2.69	2.42	1.85	0.78	1.50	1.83	0.68
13.01	2.62	0.47	0.41	3.29	3.89	1.70	2.06	1.45
13.25	2.93	1.64	0.43	2.02	5.58	1.40	2.33	1.79
13.50	4.24	1.47	2.18	1.06	2.02	0.61	1.93	1.27
13.74	4.39	20.56	5.13	3.23	4.39	2.38	6.68	6.87
13.99	3.30	5.45	2.67	1.54	0.56	1.24	2.46	1.77
14.23	-0.35	3.24	2.82	1.88	1.95	0.54	1.68	1.36
14.48	2.05	2.50	2.65	3.36	2.71	2.42	2.61	0.43
14.72	46.07	0.49	3.45	5.72	5.08	3.99	10.80	17.38
14.97	-0.37	1.79	0.44	5.61	0.54	0.49	1.42	2.17

Appendix Table 4; Jgros ERP 4-weeks; Lithium concentration measurements (ppm) over depth (µm) for 6 spots, the average, and standard deviation of all 6 spots.